Nonlinear Analysis: Modelling and Control, Vol. 20, No. 3, 455–468 ISSN 1392-5113
http://dx.doi.org/10.15388/NA.2015.3.10

Modelling of catalytic reactivity of inhomogeneous surfaces in monomer-monomer reactions*

Vladas Skakauskas[1], **Pranas Katauskis**

Faculty of Mathematics and Informatics, Vilnius University
Naugarduko str. 24, LT-03225 Vilnius, Lithuania
vladas.skakauskas@mif.vu.lt; pranas.katauskis@mif.vu.lt

Received: March 6, 2014 / **Revised:** October 15, 2014 / **Published online:** March 31, 2015

Abstract. The kinetics of a $A_1 + A_2 \rightarrow A_1A_2$ reaction on inhomogeneous surfaces with continuously distributed adsorption sites is investigated numerically using two phenomenological models. One of them includes: the bulk diffusion of reactants from a bounded vessel towards the adsorbent and the product bulk one from the adsorbent into the same vessel, adsorption and desorption of molecules of both reactants, and surface diffusion of adsorbed and product particles before their desorption. The other model describes surface reaction provided that concentrations of both reactants at the surface are given. Both models are based on the Langmuir–Hinshelwood reaction mechanism coupled with the Eley–Rideal step. Two surface diffusion mechanisms are used. According to one of them, the diffusion flux of the adsorbed and product particles is described by the standard Fick law, while in the other one the surface diffusion flux is based on the particle jumping into a nearest vacant adsorption site. Simulations were performed using the finite difference technique. The kinetic rate constants, Eley–Rideal steps, and surface diffusion mechanisms influence on the catalytic reactivity of surfaces is studied.

Keywords: heterogeneous reactions, adsorption, desorption, surface diffusion.

1 Introduction

Simulations are of central importance in study of kinetics in heterogeneous catalysis and catalysts design in chemical industry [1,2,6,7,13,14]. The bibliography of the current state of modelling in theoretical research of monomer-monomer reactions on inhomogeneous surfaces includes a lot of papers based on the Monte Carlo simulations technique and a considerably less number of works is devoted to numerical or analytical solving of mean-field models. The bibliography of papers based on the Monte Carlo simulations can

*This work was supported by the Research Council of Lithuania (project No. MIP-052/2012).
[1]Corresponding author.

be found, e.g., in [5] and [12]. Moreover, a short review of papers is given in [12]. Some mean-field models are solved numerically or studied analytically in [3, 10, 12, 13].

A common feature of the previous reports dealing with adsorption and surface reactions is that the partial pressures of both reactants at the surface are assumed to be given constants and product desorption from the surface is supposed to be instantaneous. Exclusive is paper [10] in which the distribution of adsorption sites is stepwise but both reactants diffuse towards the surface from a bounded pool.

In this paper, by employing a mean-field approach and its numerical simulations we consider two models of monomer-monomer heterogeneous reaction, $A_1 + A_2 \to B$, $B = A_1A_2$, on catalytic surfaces with continuous (not stepwise) arrangement of adsorption sites which are assumed to be active in reaction. Note that the spillover effect does not arise on the surfaces with continuously distributed adsorption sites. One model involves: (i) the bulk diffusion of both reactants from a bounded vessel with an impermeable boundary toward the adsorbent and the reaction product bulk one from the adsorbent into the same vessel, (ii) adsorption, desorption, and surface diffusion of adsorbed particles of each reactant. The other model describes surface reactions provided that concentrations of both reactants at the surface are given. Both models are based on the Langmuir–Hinshelwood surface reaction mechanism coupled with the Eley–Rideal step. In particular, models based only on the Langmuir–Hinshelwood (LH) or Eley–Rideal (ER) mechanisms are also studied. In both models, we use two surface diffusion mechanisms. According to one of them, the diffusion flux of the adsorbed and product particles is described by the standard Fick law, while in the other one the surface diffusion flux is based on the particle jumping into a nearest vacant adsorption site [4]. Adsorption, desorption, surface and bulk diffusion are allowed to proceed at a constant temperature.

The goal of this paper is the numerical study of the influence of the surface diffusion mechanisms, bulk and surface diffusivity of both reactants and surface diffusivity of product particles, desorption rate constant of product particles, adsorption sites arrangement, and the LH or ER steps on the reactivity of catalyst surfaces.

The paper is organized as follows. In Section 2, we present the models. In Section 3, we discuss numerical results. A summary of main results in Section 4 concludes the paper.

2 The model

We study the problem of two-molecular catalytic heterogeneous reaction, $A_1 + A_2 \to B$, on surfaces with continuously (nonuniformly) distributed adsorption sites by using a mean-field approach. We assume that all sites are equivalent and active in reaction so that both reactants compete for the adsorption site. Let the reactants A_1, A_2 and product $B = A_1A_2$ of concentrations $a_1(t,x)$, $a_2(t,x)$, and $b(t,x)$ occupy a bounded domain $\Omega = \{x = (x_1, x_2, x_3)\colon\ x_i \in [0,l],\ i = 1,2,3\}$ with boundary $\tilde{S} = S_1 \cup S_2$, where $S_2 = \{x = (x_1, x_2, x_3)\colon\ x_i \in [0,l],\ i = 1,3, x_2 = 0\}$ and $S_1 = \tilde{S} \setminus S_2$. Here t is time, x is a position, S_2 is the surface of the adsorbent, and S_1 is a surface impermeable to the reactants and product. It is evident that $x_2 > 0$ for S_1. Let $s(x)$ be the surface

density of the adsorption sites and let $u_i(t,x) = s(x)\theta_i(t,x)$, $i = 1,2,3$, be densities of the adsorption sites occupied by the adsorbed molecules of reactants A_1, A_2, and product B, respectively. Here θ_i is a surface coverage. Then $s(1-\theta_1-\theta_2-\theta_3)$ is density of free adsorption sites. Since, according to the Langmuir–Hinshelwood hypotheses, one reactant molecule adsorbs on only one adsorption site, functions u_1, u_2, and u_3 also present densities of adsorbed molecules at point x at time t of reactants A_1, A_2, and particles of the product B. Reaction between one molecule of reactant A_1 located in an adsorption site and one molecule of reactant A_2 located in the other adsorption site forms one product molecule located in one adsorption site. The other one becomes free. Let k_{11}, k_{21} and k_{-11}, k_{-21} be the adsorption and desorption rates constants for reactants A_1 and A_2, respectively, k_1 and k_2 – reaction rate constants in the ER reaction, k_3 – reaction rate constant in the LH reaction step. To simplify the model, we restrict ourselves to the case where the adsorption sites density, s, depends only on variable x_1 and the initial values a_{10} and a_{20} of concentrations a_1 and a_2 do not depend on x_3. In this case, we can reduce the three-dimensional problem into two-dimensional one.

In what follows, we consider the case where the product molecules desorb slowly from the catalyst surface. To construct the model, we first employ the Langmuir–Hinshelwood reaction mechanism

$$A_1 + S \underset{k_{-11}}{\overset{k_{11}}{\rightleftarrows}} A_1S, \qquad A_2 + S \underset{k_{-21}}{\overset{k_{21}}{\rightleftarrows}} A_2S, \qquad A_1S + A_2S \overset{k_3}{\to} A_1A_2S + S.$$

Here S is a free adsorption site. In principle, the product $B = A_1A_2$ may be formed via one or both Eley–Rideal steps

$$A_1 + A_2S \overset{k_1}{\to} A_1A_2S, \qquad A_2 + A_1S \overset{k_2}{\to} A_1A_2S.$$

Since product particles desorb slowly, we join the last step $A_1A_2S \overset{k_4}{\to} A_1A_2 + S$, where k_4 is a product particles desorption rate constant.

In what follows, we apply two surface diffusion mechanisms. In one of them, the diffusion flux of the adsorbed particles of the ith species is described by the standard Fick law,

$$J_i = -\kappa_{u_i}\nabla u_i \tag{1}$$

with constant surface diffusivity κ_{u_i}, $i = 1,2,3$, while in the other one the surface diffusion flux is based on the mechanism of the particle jumping into a nearest vacant adsorption site [4],

$$J_i = -\tilde{\kappa}_{u_i}\big((s-u_1-u_2-u_3)\nabla u_i - u_i\nabla(s-u_1-u_2-u_3)\big). \tag{2}$$

Here ∇ is the gradient operator and $\tilde{\kappa}_{u_i}$, $i = 1,2,3$, is a constant surface diffusion coefficient. According to formula (2), flux J_i is sum of two fluxes. One of them is proportional

to $-\nabla u_i$ while the other one is proportional to the gradient of the free adsorption sites. To derive equations for densities u_1, u_2, u_3, we employ the mass action law and Eqs. (1) and (2), getting

$$\begin{aligned}
\partial_t u_1 &= k_{11}a_1\left(s-\sum_{j=1}^{3}u_j\right)-k_{-11}u_1-k_3u_1u_2-k_2a_2u_1+\kappa_{u_1}\frac{\partial^2 u_1}{\partial x_1^2},\\
\partial_t u_2 &= k_{21}a_2\left(s-\sum_{j=1}^{3}u_j\right)-k_{-21}u_2-k_3u_1u_2-k_1a_1u_2+\kappa_{u_2}\frac{\partial^2 u_2}{\partial x_1^2},\\
\partial_t u_3 &= k_3u_1u_2+k_1u_2a_1+k_2u_1a_2-k_4u_3+\kappa_{u_3}\frac{\partial^2 u_3}{\partial x_1^2}
\end{aligned} \tag{3}$$

in the case of Eq. (1) and

$$\begin{aligned}
\partial_t u_1 &= k_{11}a_1\left(s-\sum_{j=1}^{3}u_j\right)-k_{-11}u_1-k_3u_1u_2-k_2a_2u_1\\
&\quad+\tilde{\kappa}_{u_1}\left((s-u_2-u_3)\frac{\partial^2 u_1}{\partial x_1^2}-u_1\frac{\partial^2(s-u_2-u_3)}{\partial x_1^2}\right),\\
\partial_t u_2 &= k_{21}a_2\left(s-\sum_{j=1}^{3}u_j\right)-k_{-21}u_2-k_3u_1u_2-k_1a_1u_2\\
&\quad+\tilde{\kappa}_{u_2}\left((s-u_1-u_3)\frac{\partial^2 u_2}{\partial x_1^2}-u_2\frac{\partial^2(s-u_1-u_3)}{\partial x_1^2}\right),\\
\partial_t u_3 &= k_3u_1u_2+k_1u_2a_1+k_2u_1a_2-k_4u_3\\
&\quad+\tilde{\kappa}_{u_3}\left((s-u_2-u_1)\frac{\partial^2 u_3}{\partial x_1^2}-u_3\frac{\partial^2(s-u_2-u_1)}{\partial x_1^2}\right)
\end{aligned} \tag{4}$$

in the case of Eq. (2). Here $x_1\in(0,l)$, $x_2=0$, $t>0$, and ∂_t signifies the partial derivative with respect to time.

We add to systems (3) and (4) the initial

$$u_1|_{t=0}=u_2|_{t=0}=u_3|_{t=0}=0 \tag{5}$$

and boundary conditions at points $x_1=0$ and $x_1=l$,

$$\frac{\partial u_1}{\partial x_1}=\frac{\partial u_2}{\partial x_1}=\frac{\partial u_3}{\partial x_1}=0,\quad t>0. \tag{6}$$

We also formulate the conditions $\partial s/\partial x_1=0$ at points $x_1=0$ and $x_1=l$. Systems (3) and (4) involve unknown values of concentrations a_1 and a_2 at the catalyst surface. To close these systems, we add equations for the bulk diffusion of both reactants.

Diffusion of the reactants A_1 and A_2 toward the adsorbent and the product B from the adsorbent away into the same vessel is described by the systems:

$$\begin{aligned}
&\partial_t a_1 = \kappa_{a_1}\left(\frac{\partial^2 a_1}{\partial x_1^2} + \frac{\partial^2 a_1}{\partial x_2^2}\right), \quad (x_1, x_2) \in (0,l)\times(0,l),\ t>0,\\
&\partial_n a_1|_{S_1} = 0, \quad t>0,\\
&\kappa_{a_1}\partial_n a_1|_{S_2} = -\left(k_{11}a_1\left(s - \sum_{j=1}^{3} u_j\right) - k_{-11}u_1 + k_1 a_1 u_2\right)\Bigg|_{S_2}, \quad t>0,\\
&a_1|_{t=0} = a_{10}, \quad (x_1, x_2) \in (0,l)\times(0,l),
\end{aligned} \tag{7}$$

$$\begin{aligned}
&\partial_t a_2 = \kappa_{a_2}\left(\frac{\partial^2 a_2}{\partial x_1^2} + \frac{\partial^2 a_2}{\partial x_2^2}\right), \quad (x_1, x_2) \in (0,l)\times(0,l),\ t>0,\\
&\partial_n a_2|_{S_1} = 0, \quad t>0,\\
&\kappa_{a_2}\partial_n a_2|_{S_2} = -\left(k_{21}a_2\left(s - \sum_{j=1}^{3} u_j\right) - k_{-21}u_2 + k_2 a_2 u_1\right)\Bigg|_{S_2}, \quad t>0,\\
&a_2|_{t=0} = a_{20}, \quad (x_1, x_2) \in (0,l)\times(0,l),
\end{aligned} \tag{8}$$

and

$$\begin{aligned}
&\partial_t b = \kappa_b\left(\frac{\partial^2 b}{\partial x_1^2} + \frac{\partial^2 b}{\partial x_2^2}\right), \quad (x_1, x_2) \in (0,l)\times(0,l),\\
&\partial_n b|_{S_1} = 0, \quad t>0,\\
&\kappa_b\partial_n b|_{S_2} = k_4 u_3|_{S_2}, \quad t>0,\\
&b|_{t=0} = 0, \quad (x_1, x_2) \in (0,l)\times(0,l).
\end{aligned} \tag{9}$$

Here $\partial_n f$, $f = a_1, a_2, b$, is the outward normal derivative. Each of systems (3), (5)–(9) and (4)–(9) possess two mass conservation laws

$$\int_\Omega (a_i + b)\,\mathrm{d}x + \int_0^l (u_i + u_3)\,\mathrm{d}x_1 = \int_\Omega a_{i0}\,\mathrm{d}x, \quad i = 1,2, \tag{10}$$

and determines densities u_i (or surface coverages θ_i) for all $x \in S_2$ and concentrations a_1, a_2, and b of reactants A_1, A_2, and product B for all $(x_1, x_2) \in (0,l)\times(0,l)$ and $t>0$.

We also study systems (3) and (4) with given constant concentrations a_1 and a_2 at the surface S_2. In the case of constant s and positive kinetic coefficients, the unique solutions of systems (3) and (4) asymptotically tend to the positive steady-state point,

$$\begin{aligned}
&u_1 = \frac{1}{2q_1q_5}(h_1 + \sqrt{h_1^2 + h_2}), \qquad u_2 = \frac{sk_{11}a_1 - q_3u_1}{q_4 + q_5u_1},\\
&u_3 = \frac{1}{k_4}(k_3u_1u_2 + k_1u_2a_1 + k_2u_1a_2),
\end{aligned}$$

where

$$
\begin{aligned}
h_1 &= sq_0q_5 - q_1q_4 + q_2q_3,\\
h_2 &= 4sq_1q_5k_{11}a_1k_3(k_{-21} + k_1a_1)\left(1 + \frac{k_{11}a_1}{k_4}\right),\\
q_0 &= k_3(k_{11}a_1 - k_{21}a_2),\\
q_1 &= \left(1 + \frac{k_2a_2}{k_4}\right)q_0 + k_3\left(1 + \frac{k_{21}a_2}{k_4}\right)(k_{-11} + k_2a_2),\\
q_2 &= \left(1 + \frac{k_1a_1}{k_4}\right)q_0 - k_3\left(1 + \frac{k_{11}a_1}{k_4}\right)(k_{-21} + k_1a_1),\\
q_3 &= k_{11}a_1\left(1 + \frac{k_2a_2}{k_4}\right) + k_{-11} + k_2a_2,\\
q_4 &= k_{11}a_1\left(1 + \frac{k_1a_1}{k_4}\right), \qquad q_5 = k_3\left(1 + \frac{k_{11}a_1}{k_4}\right).
\end{aligned}
$$

The main characteristic that we study in this paper is the surface S_2 specific conversion rate of molecules of both reactants into the product ones (turn-over rate or turn-over frequency) determined by the formula

$$z = \frac{\int_0^l k_4u_3\,\mathrm{d}x_1}{\int_0^l s\,\mathrm{d}x_1}. \tag{11}$$

We also study the other function

$$z_1 = \frac{\int_0^l (k_3u_1u_2 + k_1a_1u_2 + k_2a_2u_1)\,\mathrm{d}x_1}{\int_0^l s\,\mathrm{d}x_1} \tag{12}$$

which describes the specific conversion rate of molecules of both reactants into product ones but before their desorption from the surface S_2.

In the case where $k_{11}a_1 = k_{21}a_2$ and $s = \mathrm{const}$, from the steady-state version of system (3) it follows that (i) $u_1 = s$, $u_2 = u_3 = 0$ if $k_{-11} = k_2 = 0$ and (ii) $u_2 = s$, $u_1 = u_3 = 0$ if $k_{-21} = k_1 = 0$. Hence, by definition, z_1 and z are equal to zero. Applying the Lienard–Chipard criterion [8] it is easy to prove that these steady-state points are asymptotically stable. This means that the catalyst surface becomes poisoned by reactant A_1 or A_2. Numerical experiments show that z and z_1 increase in time, reach maximal values, and then tend to zero.

In the case of only one ER step ($k_3 = 0$), from system (3) it follows (mathematically strongly) that z and z_1 do not depend on the specific continuous adsorption sites distribution preserving the same $\int_0^1 s(x_1)\,\mathrm{d}x_1$. Numerical experiments (see next section) exhibit the same result for the LH or coupled LH and ER reaction mechanisms.

Using the dimensionless variables $\bar{t} = t/T$, $\bar{x}_i = x_i/l$, $\bar{a}_i = a_i/a_*$, $\bar{s} = s/(la_*)$, $\bar{k}_{i1} = k_{i1}Ta_*$, $\bar{k}_{-i1} = k_{-i1}T$, $\bar{k}_3 = k_3T$, $\bar{k}_i = k_iTa_*$, $\bar{\kappa}_{a_i} = \kappa_{a_i}T/l^2$, $\bar{\kappa}_b = \kappa_bT/l^2$,

$\bar{\tilde{\kappa}}_{u_j} = \tilde{\kappa}_{u_j} a_* T/l$, $\bar{u}_j = u_j/(la_*)$, $\bar{\kappa}_{u_j} = \kappa_{u_j} T/l^2$, where $i = 1, 2$, $j = 1, 2, 3$, and T, l, a_* are the characteristic dimensional units, we rewrite Eqs. (3)–(9) in the same form, but in dimensionless variables.

3 Numerical results

To solve systems (3) and (4) with given values of a_1 and a_2 at the surface S_2, we applied an implicit difference scheme. Systems (3), (5)–(9) and (4)–(9) were solved by using an implicit difference scheme based on the alternating direction method [9]. For all calculations, we used the following dimensional data: $T = 1$ s, $l = 10^{-1}$ cm, $a_* = 10^{-11}$ mol cm^{-3}, $s_* = la_* = 10^{-12}$ mol cm^{-2}, and

$$\begin{aligned} &k_{i1} \in \left[10^9, 10^{11}\right] \text{ cm}^3 \text{ mol}^{-1} \text{ s}^{-1}, \qquad k_{-i1}, k_3 \in \left[3 \cdot 10^{-3}, 1\right] \text{ s}^{-1}, \\ &\kappa_{a_i}, \kappa_b, \kappa_{u_j} \in \left[5 \cdot 10^{-7}, 10^{-3}\right] \text{ cm}^2 \text{ s}^{-1}, \end{aligned} \tag{13}$$

where $i = 1, 2$, $j = 1, 2, 3$. The range of kinetic parameters given in (13) was taken from [11] while the other parameters are the model ones. Particles of size 10^{-1} cm can be used in the design of the supported catalysts. In the case where values of k_{i1}, κ_{u_i}, κ_{a_i} for all values of indices are equal, we use $k = k_{i1}$, $\kappa_u = \kappa_{u_i}$, $\kappa_a = \kappa_{a_i}$ for short. Of course, the case where k_{i1}, κ_{u_i} do not depend on values of indices is not realistic. However, it is useful for study of many different physico-chemical processes. In calculations, we used $k = 0.0166$, $k_1 = k_2 = 0.5k_{11}$ or 0, and $\tilde{\kappa}_{u_i} = \kappa_{u_i}$ (dimensional surface diffusion coefficients are different), and

$$s = \frac{1}{2}\left(\sin^2 \frac{m\pi x_1}{2} + 1\right) \quad \text{with natural } m$$

and

$$\int_0^1 s(x_1)\,\mathrm{d}x_1 = 0.75 \quad \text{or} \quad s = 0.75,$$

$$a_{10} = \frac{(1 + \alpha_{11}\sin^2(\pi x_1))(1 + \alpha_{12}\sin(\pi x_2/2))}{1 + 0.5\alpha_{11}} \frac{1 + 2\alpha_{12}}{\pi},$$

$$a_{20} = \frac{(1 + \alpha_{21}\sin^2(\pi x_1))(1 + \alpha_{22}\sin(\pi x_2/2))}{1 + 0.5\alpha_{21}} \frac{1 + 2\alpha_{22}}{\pi}$$

with $\alpha_{ij} = 1$. The model values of dimensionless k_{i1}, κ_{u_i} are given in the captions of figures. The use of initial functions of this type was motivated by the intention to get an appreciable influence of the bulk diffusion of both reactants in the initial stage, i.e., to have the initial distribution being far from of the equilibrium. Numerical results are illustrated in Figs. 1–7 with $\kappa_u = 1$ for Figs. 1, 2, $\tilde{\kappa}_u = \kappa_u = 0.5$ for Figs. 3, 4, and $\kappa_u = 0.5$ for Figs. 5–7. Plots in Figs. 1 and 2 correspond to system (3), (5)–(9). The comparison of z determined by systems (3), (5)–(9) and (4)–(9) is given in Fig. 3, while Fig. 4 shows the

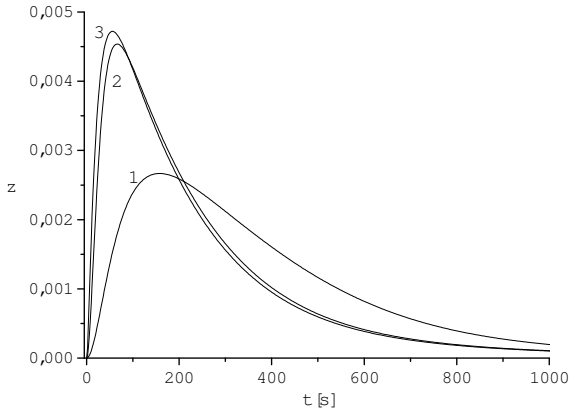

Fig. 1. Influence of product desorption rate constant k_4 on the behaviour of the turn-over rate z determined by system (3), (5)–(9) for $k_1 = k_2 = 0.5k_{11}$, $k_3 = 0.03$, $k_{-11} = k_{-21} = 0.00166$, $\kappa_a = 0.1$. $k_4 = 0.01$ (1), 0.1 (2), 0.5 (3).

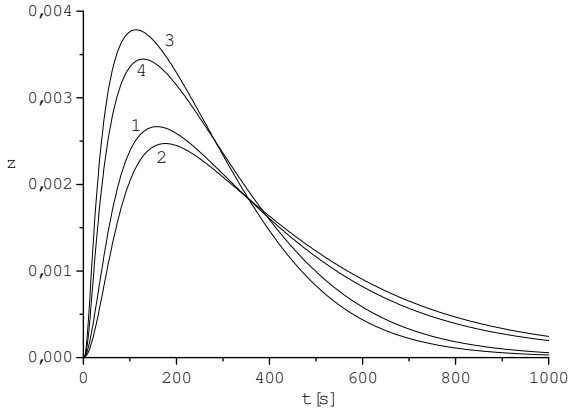

Fig. 2. Dependence of z from system (3), (5)–(9) on the diffusivity κ_a and constant k_3 for $k_1 = k_2 = 0.5k_{11}$, $k_4 = 0.01$, $k_{-11} = k_{-21} = 0.00166$. $k_3 = 0.03$, $\kappa_a = 0.1$ (1) and 0.01 (2); $k_3 = 1$, $\kappa_a = 0.1$ (3) and 0.01 (4).

comparison of z corresponding to systems (3) and (4) with given a_1 and a_2 at the catalyst surface. Figures 5–7 correspond to system (3) with given concentrations a_1 and a_2 at the catalyst surface.

Figure 1 illustrates the dependence of the turn-over rate z on the product desorption rate constant k_4 for the case where $k_1 = k_2 = 0.5k_{11}$, $k_3 = 0.03$, $k_{-11} = k_{-21} = 0.00166$, $\kappa_a = 0.1$. For small time, Fig. 1 depicts a notable decrease of the turn-over rate z as product desorption rate constant, k_4, decreases and a vice-versa behaviour as time increases. This effect is evident because the product particles poison the catalyst. This leads to a smaller uptake of reactants in the vessel compared to that corresponding to a larger k_4 and, hence, reaction proceed longer.

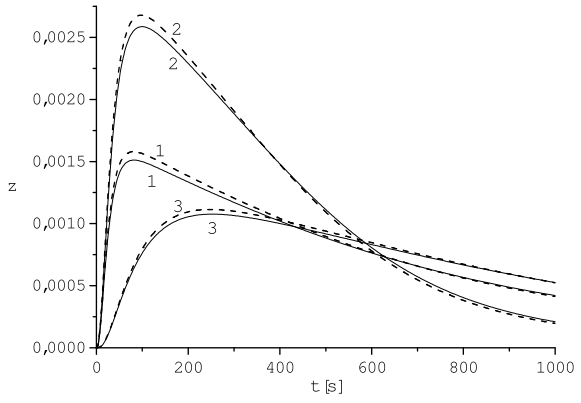

(a)

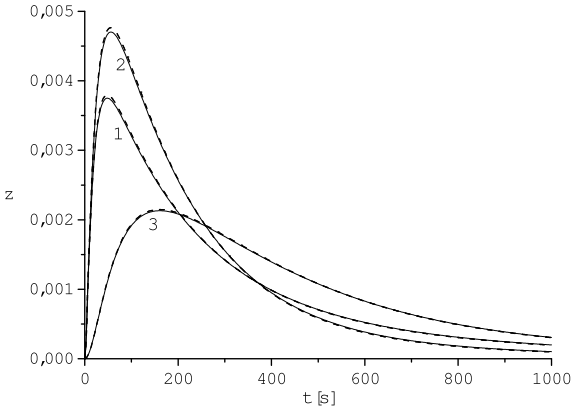

(b)

Fig. 3. Effect of surface diffusion mechanisms (solid line – system (3), (5)–(9), dashed line – system (4)–(9)) and parameter $k_1 = k_2$ on the function z: $k_1 = k_2 = 0$ (a), $k_1 = k_2 = 0.5k_{11}$ (b). $k_4 = 0.5$, $k_{-11} = k_{-21} = 0.0166$ (1) and $k_{-11} = k_{-21} = 0.00166$ (2); $k_4 = 0.01$, $k_{-11} = k_{-21} = 0.0166$ (3) with $\kappa_a = 0.1$ and $k_3 = 0.03$.

Figure 2 depicts the influence of the bulk diffusivity κ_a and reaction rate constant k_3 in the LH step on the behaviour of z for the case where $k_1 = k_2 = 0.5k_{11}$, $k_4 = 0.01$, $k_{-11} = k_{-21} = 0.00166$. From this figure we see that, for small time, the growth of k_3 or κ_a increases z. But for large time, it behaves vice-versa. To clarify this effect, the argument used for explanation of the effect discussed in Fig. 1 can be also applied.

Figure 3 presents the comparison of the dependence of z determined by systems (3), (5)–(9) and (4)–(9) on the parameter $k_1 = k_2$ which is equal to zero in Fig. 3a and to $0.5k_{11}$ in Fig. 3b. To construct both figures, we used $k_3 = 0.03$ and $\kappa_a = 0.1$. Values of the other parameters are as follows: $k_4 = 0.5$, $k_{-11} = k_{-21} = 0.0166$ for curves 1, $k_4 = 0.5$, $k_{-11} = k_{-21} = 0.00166$ for curves 2, $k_4 = 0.01$, $k_{-11} = k_{-21} = 0.0166$ for curves 3. We see that, for small time, the function z grows as $k_{-11} = k_{-21}$ decreases and

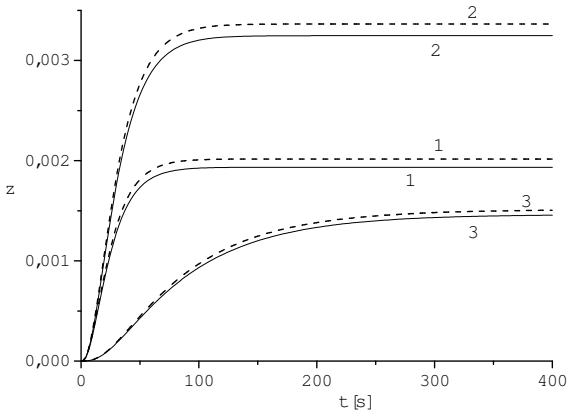

Fig. 4. Effect of surface diffusion mechanisms (solid line – system (3), dashed line – system (4) with $a_1 = a_2 = 1$) and parameters k_4 and $k_{-11} = k_{-21}$ on z in case of $k_1 = k_2 = 0$ and $k_3 = 0.03$: $k_4 = 0.5$, $k_{-11} = k_{-21} = 0.0166$ (1) and $k_{-11} = k_{-21} = 0.00166$ (2); $k_4 = 0.01$, $k_{-11} = k_{-21} = 0.0166$ (3).

behaves vice-versa for long time. For small time, this effect is obvious due to growing number of reacting particles. The long-time behaviour of z can be explained by applying the argument used for Figs. 1 and 2. Comparison of plots depicted in these figures shows that involving of the ER step for one or both reactants remarkably increases z compared to that corresponding to the model based only on the LH mechanism.

Plots in Fig. 3 also demonstrate the influence of two different surface diffusion mechanisms on the the behaviour of z determined by systems (3), (5)–(9) and (4)–(9). The diffusion mechanism [4] increases z only for small time and slightly decreases it for large time. This increase is appreciable only in the case of the absence of the ER steps (compare both Figs. 3). Calculations show that maximal increase is about 5.5–6.3%.

Figure 4 illustrates the influence of two surface diffusion mechanisms and parameters k_4 and $k_{-11} = k_{-21}$ on the behaviour of z determined by systems (3) and (4) with given a_1 and a_2 in the case of the absence of the ER steps. All plots corresponding to both diffusion mechanisms are monotonic in time. As in Fig. 3, the diffusion mechanism [4] increases values of z. Maximal increase is about 5%.

Plots in Fig. 5 illustrate the dependence of z on k_3, k_4, and $k_{-11} = k_{-21}$. Fig. 5a corresponds to $k_1 = k_2 = 0$, $k_3 = 0.03$ (solid line) and $k_3 = 0.01$ (dashed line). In Fig. 5b, all plots correspond to $k_1 = k_2 = 0.5k_{11}$, $k_3 = 0.03$ (solid line) and $k_3 = 0$ (dashed line). Values of the other parameters are as follows: $k_4 = 0.5$, $k_{-11} = k_{-21} = 0.0166$ for curve 1 and $k_{-11} = k_{-21} = 0.00166$ for curve 2, $k_4 = 0.01$, $k_{-11} = k_{-21} = 0.0166$ for curve 3. We stress that in the case where $k_3 = 0$ reaction occurs via only ER steps while in the case where $k_1 = k_2 = 0$ reaction is governed by the LH mechanism. Figure 4 shows that, for $k_1 = k_2$, z monotonically tends in time to asymptotic values depending on parameters under consideration and decreases as k_4 decreases or $k_{-11} = k_{-21}$ increases.

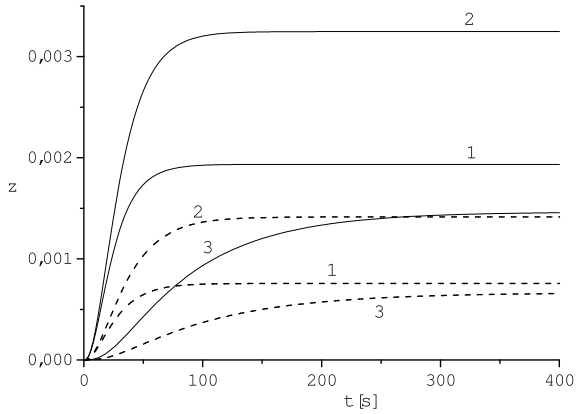

(a)

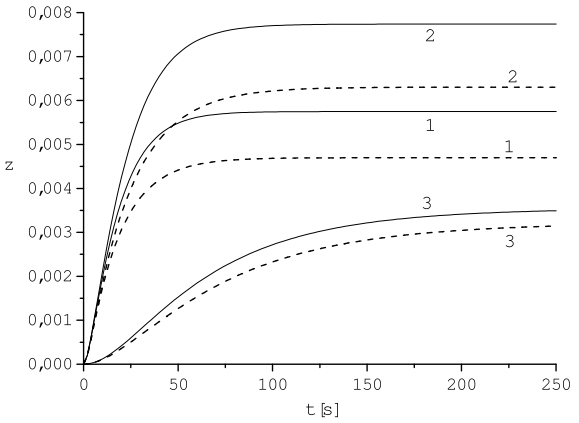

(b)

Fig. 5. Influence of parameters k_3, k_4, and $k_{-11} = k_{-21}$ on the behaviour of z determined by system (3) with $a_1 = a_2 = 1$: (a) $k_1 = k_2 = 0$, $k_3 = 0.03$ (solid line) and $k_3 = 0.01$ (dashed line), (b) $k_1 = k_2 = 0.5k_{11}$, $k_3 = 0.03$ (solid line) and $k_3 = 0$ (dashed line). $k_4 = 0.5$, $k_{-11} = k_{-21} = 0.0166$ (1) and $k_{-11} = k_{-21} = 0.00166$ (2); $k_4 = 0.01$, $k_{-11} = k_{-21} = 0.0166$ (3).

Figure 6 depicts the influence of parameters k_2, k_{-11}, k_{-21}, and k_4 on the behaviour of z for $k_3 = 0.03$ in the cases $k_1 = k_2 = 0$ (solid line) and $k_1 = 0$, $k_2 = 0.5k_{11}$ (dashed line). Values of the other parameters are the same as those used for Fig. 5. This figure shows that in case of $k_1 = 0$, $k_2 = 0.5k_{11}$ and large k_4, function z is non-monotonic in time. It increases, reaches a maximum value, which grows as $k_{-11} = k_{-21}$ decreases, and then tends to an asymptotic value that is smaller than that corresponding to a larger value of $k_{-11} = k_{-21}$.

Calculations show that z determined by system (3), (5)–(9) with constant initial concentrations of both reactants and z_1 determined by Eqs. (3) with given constant

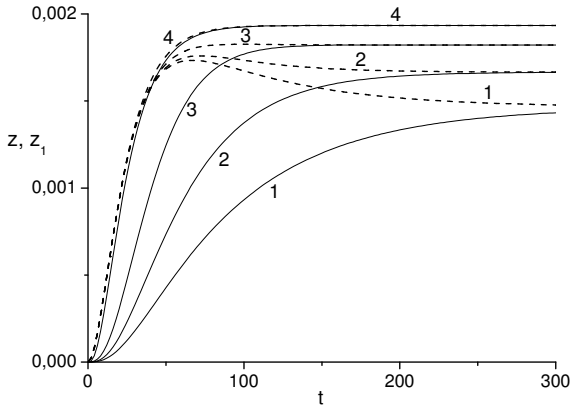

Fig. 6. Influence of k_1, k_2, $k_{-11} = k_{-21}$, and k_4 on z from system (3) with $a_1 = a_2 = 1$ for $k_3 = 0.03$ in the cases $k_1 = k_2 = 0$ (solid line) and $k_1 = 0$, $k_2 = 0.5k_{11}$ (dashed line). $k_4 = 0.5$, $k_{-11} = k_{-21} = 0.0166$ (1) and $k_{-11} = k_{-21} = 0.00166$ (2); $k_4 = 0.01$, $k_{-11} = k_{-21} = 0.0166$ (3).

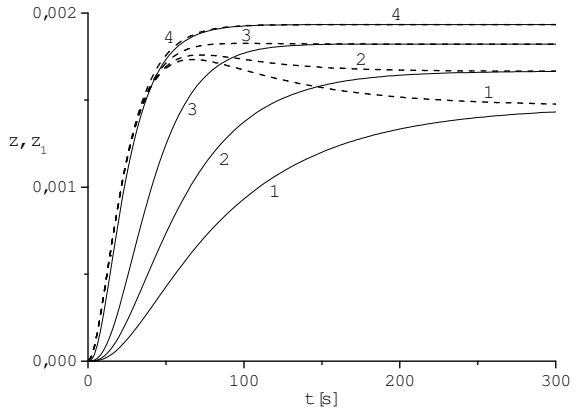

Fig. 7. Comparison of z (solid line) and z_1 (dashed line) determined by Eqs. (3) with $a_1 = a_2 = 1$ at the catalyst surface for different values of k_4: 0.01 (1), 0.02 (2), 0.05 (3), 0.5 (4) for $k_3 = 0.03$, $k_1 = k_2 = 0$ and $k_{-11} = k_{-21} = 0.0166$.

concentrations a_1 and a_2 do not depend on the natural parameter m involved in the definition of $s(x_1)$ which preserves the same total number of adsorption sites and practically do not depend of the diffusivity κ_u. The same result was also achieved for $s = 0.75$. As we mentioned in Section 2, in the case of only one ER step, the independence of z and z_1 on the specific type of s can be proved strongly.

Fig. 7 illustrates a convergence of z towards z_1 as the product desorption rate constant, k_4, increases. This figure also shows that function z_1 is non-monotonic in time for small k_4 and practically is independent of k_4 for small time.

4 Conclusions

To conclude the paper, we summarise the main results. In this paper, using a phenomenological (mean-field) approach in two-dimensional space, we studied numerically the model of monomer-monomer surface reactions proceeding on the inhomogeneous catalytic surfaces coupled with the bulk diffusion of both reactants from the bounded vessel towards the surface and the product bulk one from the surface into the same vessel. Adsorption, desorption, and surface diffusion of the adsorbed and product particles and a slow product desorption are taken into account. To describe the surface diffusion, two different mechanisms were used: (i) the standard Fick law with a constant diffusivity, (ii) the mechanism based on the particle jumping into a nearest vacant site [4]. The model where densities of both reactants at the surface are given is also studied.

The main characteristic we studied was the catalytic surface specific conversion rate (turn-over rate) of molecules of both reactants into the product ones. We analysed effects of the desorption rate constants of adsorbed and product particles, bulk diffusivity of reactants and mechanism of surface diffusion of both adsorbates and product particles, reaction rate constants in the LH and ER steps on the turn-over rate and demonstrated that:

1. In both models, the additional ER step for one or both reactants dramatically increases the turn-over rate z compared to that corresponding to only one LH mechanism.
2. In models (3), (5)–(9) and (4)–(9), the slow desorption of product particles remarkably changes (decreases for small time but increases for long time) the turn-over rate z. This is because the product particles poison the catalyst. This leads to a smaller uptake of reactants in the vessel compared to that corresponding to a larger value of k_4 and, hence, reaction proceeds longer in case of small k_4.

   In models (3) and (4) with given concentrations of both reactants at the catalyst surface, the slow desorption of product particles decreases z for all time. In the case of these systems, the product particles also poison the catalyst surface but the supply of reactants particles is constant.
3. Function z for system (3) or (4) with given a_1 and a_2 at the surface S_2 is monotonic in time for $k_1 = k_2 \geqslant 0$ and non-monotonic if only one of k_1 and k_2 is zero and k_4 is large. In the latter case, z corresponding to system (3) or (4) and z corresponding to Eqs. (3), (5)–(9) or (4)–(9) with $k_1 = k_2 \geqslant 0$ attain maximum values depending on k_4 and the other parameters and then tend to positive asymptotic values (in case of systems (3), (4)) or zero (in case of systems (3), (5)–(9) or (4)–(9)) as time grows. In case of systems (3), (5)–(9) and (4)–(9), z grows only for small t and behaves vice versa for large t. If one of k_1 or k_2 is equal to zero and product desorption rate constant, k_4, is large, then z corresponding to system (3) or z determined by (4) grow for small time, attain maximal values and then decrease to positive asymptotic values.
4. z and z_1 determined by systems (3), (5)–(9), (4)–(9), and (3), (4) for large time are practically independent of κ_{u_i}, $i = 1, 2, 3$, and specific continuous (not stepwise)

distribution of adsorption sites, $s(x_1)$, which preserves the same total number of adsorption ones.

5. The increase of at least one of k_3, k_4, κ_{a_1}, κ_{a_2}, or decrease of $k_{-11} = k_{-21}$ increases $z(t)$ determined by system (3), (5)–(9) or (4)–(9) and the increase of k_3 or decrease of $k_{-11} = k_{-21}$ increases z corresponding to systems (3) or (4).
6. The diffusion mechanism based on the particle jumping into the nearest vacant site [4] increases z compared to that corresponding to the the Fick law only for small time and slightly decreases z for large time.

References

1. A. Andrease, H. Lynggaard, C. Stegelmann, P. Stoltze, Analysis of simple kinetic models in heterogeneous catalysis, *Prog. Surf. Sci.*, **77**(3–4):71–137, 2004.
2. L.J. Broadbelt, R.Q. Snurr, Applications of molecular modeling in heterogeneous catalysis research, *Appl. Catal. A-Gen.*, **200**:23–46, 2000.
3. E. Clement, P. Leroux-Hugon, L.M. Sandler, Exact results for a chemical reaction model, *Phys. Rev. Lett.*, **67**:1661–1664, 1991.
4. A.N. Gorban, H.P. Sargsyan, H.A. Wahab, Quasichemical models of multicomponent nonlinear diffusion, *Math. Model. Nat. Phenom.*, **6**(5):184–262, 2011.
5. A. Maltz, E.V. Albano, Kinetic phase transitions in dimer-dimer surface reaction models studied by means of mean-field and Monte Carlo methods, *Surf. Sci.*, **277**:414–428, 1992.
6. T.G. Mattos, F.D.A. Aarão Reis, Effects of diffusion and particle size in a kinetic model of catalyzed reactions, *J. Catal.*, **263**:67–74, 2009.
7. D.Y. Murzin, *Ind. Eng. Chem. Res.*, On surface heterogeneity and catalytic kinetics, **44**:1688–1697, 2005.
8. A.G. Mazko, *Matrix Equations, Spectral Problems and Stability of Dynamical Systems*, Cambridge Scientific Publishers, Cottenham, 2008.
9. A.A. Samarskii, *The Theory of Difference Schemes*, Marcel Dekker, New York, 2001.
10. V. Skakauskas, P. Katauskis, Spillover in monomer-monomer reactions on supported catalysts – dynamic mean-field study, *J. Math. Chem.*, **52**(5):1350–1363, 2014.
11. V.P. Zhdanov, Arrhenius parameters for rate-processes on solid-surfaces, *Surf. Sci. Rep.*, **12**:183–242, 1991.
12. V.P. Zhdanov, B. Kasemo, Kinetic phase transitions in simple reactions on solid surfaces, *Surf. Sci. Rep.*, **20**:111–189, 1994.
13. V.P. Zhdanov, B. Kasemo, Kinetics of rapid heterogeneous reactions on the nanometer scale, *J. Catal.*, **170**:377–389, 1997.
14. V.P. Zhdanov, B. Kasemo, *Surf. Sci. Rep.*, Simulations of the reaction kinetics on nanometer supported catalyst particles, **39**:25–104, 2000.